Comparison of local structure measurements from *c*-axis polarized XAFS between a film and a single crystal of $YBa_2Cu_3O_{7-\delta}$ as a function of temperature

C. H. Booth and F. Bridges
Department of Physics, University of California, Santa Cruz, California 95064

J. B. Boyce
Xerox Palo Alto Research Center, Palo Alto, California 94304

T. Claeson
Department of Physics, Chalmers University of Technology, S-41296 Gothenburg, Sweden

B. M. Lairson
Materials Science Program, Rice University, Houston, Texas 77251

R. Liang and D. A. Bonn
Department of Physics, University of British Columbia, Vancouver, British Columbia, Canada V6T 1Z1
(Received 29 January 1996; revised manuscript received 16 May 1996)

We have performed fluorescence x-ray-absorption fine-structure (XAFS) measurements from 20–200 K on a 5000-Å *c*-axis film of $YBa_2Cu_3O_{7-\delta}$ (YBCO) on MgO (T_c=89 K) using photons polarized perpendicular to the film. The quality of the data is high out to 16 $Å^{-1}$. The data from 3–15.5 $Å^{-1}$ were transformed into *r* space and fit to a sum of theoretical standards out to 4.0 Å. These data are compared to YBCO data from a single crystal and from a film on $LaAlO_3$ with the same T_c. The main difference between the single crystal and the film data is that while the single-crystal data are well described by a two-site axial oxygen [O(4)] distribution, we see no evidence for such a distribution in either thin-film sample. We place an upper limit on the size of the axial oxygen distribution splitting for the film on MgO at $\Delta_r \lesssim 0.09$ Å. Therefore, the magnitude of any possible splitting is not directly related to T_c. Fits to the temperature-dependent data from the YBCO film on MgO indicate that all bonds show a smooth change of their broadening factor σ, except the Cu-O(4) bonds, which show an increase in σ in the vicinity of T_c, followed by a decrease of the same magnitude. Such a feature does not occur in diffraction measurements. Since XAFS measurements of σ include any correlation between the atoms in a given bond, we conclude that the O(4) position becomes less correlated with the Cu positions near T_c. Correlation measurements of these and several further near neighbors are also reported. [S0163-1829(96)07437-1]

I. INTRODUCTION

Since the discovery of the high-T_c superconductors[1] there have been several measurements of possible structural changes near the superconducting transition. Some measurements were far enough above the noise that the result was immediately convincing to the scientific community, such as the ion channeling measurements of Sharma *et al.* of a sudden correlation of the alignment in the *ab* plane of the Cu(1) (''chain copper''), O(4) (''axial oxygen''), and Cu(2) (''plane copper'') atoms in $ErBa_2Cu_3O_7$ (Ref. 2) and in $YBa_2Cu_3O_{7-\delta}$ (YBCO).[3] Some have relied on relatively small changes in a relatively large signal, such as the diffraction measurement of Horn *et al.* of an anomaly in the orthorhombicity $[(b-a)/(b+a)]$ of YBCO,[4] or the x-ray-absorption fine-structure (XAFS) measurement of Mustre de Leon *et al.* of a split O(4) position distribution ($\delta r \simeq 0.13$ Å) in YBCO that decreases somewhat or disappears ($\delta r \lesssim 0.11$ Å) near T_c.[5,6] Both of these measurements were initially treated with a fair amount of skepticism, because obtaining a reliable signal for measuring such small changes is difficult. The result of Horn *et al.* has since been confirmed both by diffraction[7] and by capacitive dilatometry measurements[8] and consequently must be considered real, although its relation to T_c is still unclear. On the other hand, the measurement of Mustre de Leon *et al.* has only been partially confirmed by XAFS (Ref. 9) (see below), and no other experiment has been able to verify the result in YBCO.

The XAFS measurement of a split O(4) site distribution has been taken as a possible explanation for anomalous features in vibrational spectra involving the O(4).[10] This distribution may also fit into current polaron models for electron-phonon-coupling (for instance, see Refs. 11–14). In spite of these important implications, the possibly dynamic nature of the O(4) distribution has never been verified. In fact, it has been suggested that the split distribution is actually due to ordered O(1) vacancies,[15] as in the Ortho-II phase of YBCO.[16,17] Part of the ambiguity in the interpretation lies in the difficulty of the measurement itself. The most serious problems with the XAFS measurements are pointed out by Stern *et al.*[9] In their attempt to confirm the measurements of Mustre de Leon *et al.*, they tried several samples with various oxygen concentrations. The only sample that was clearly consistent with a split distribution of the O(4) position had

the lowest T_c of the samples measured (89 K). Fits to a split distribution for the other samples were less convincing; both the single-site fit and the split-site fit were unsatisfactory. The sample with the highest T_c (92 K) did not show any temperature dependence near T_c, at least as far as the fits were concerned. Since the measurement relies on such a small change in the overall signal and the results were severely sample dependent, the authors concluded that an independent method is necessary to confirm the split-site character of the O(4) distribution. They also concluded that the relation between the split distribution and T_c must be weak and unimportant to superconductivity since the highest T_c sample showed the least change with temperature. This conclusion is weak, however, because the fits to this $T_c=92$ K sample were of poor quality.

Unfortunately, no independent experiments have been able to confirm the result in YBCO, although x-ray-diffraction analysis has seen a much larger effect in single crystals of $YBa_2Cu_{2.78}O_7$,[18] pulsed neutron diffraction (using a pair-distribution function analysis[19]) has seen correlated displacements of the Cu and axial oxygen in Tl-2212, and XAFS has seen axial oxygen changes near T_c in Tl-1234.[20]

As Stern *et al.* have pointed out, until an independent experiment confirms or refutes the possibly split nature of the O(4) position, the split nature of the O(4) site will be questionable. However, with different samples, analysis techniques, etc., XAFS can still help clarify the issue. For instance, well oriented samples are important for these XAFS measurements because the polarization of the incoming synchrotron light can be utilized to remove the contribution to the XAFS of the in-plane oxygens. Magnetically oriented powders were used in the studies of both Mustre de Leon *et al.* and Stern *et al.* Each of these absorption measurements were made in the transmission mode. In the study presented here, we use a 5000-Å film on MgO, a 4000-Å film on $LaAlO_3$, and a 17-μm (1.4% Ni substitutes for Cu) single crystal of YBCO, all with a T_c of 89 K. Each of these samples is highly oriented with the c axis perpendicular to the sample surface. All measurements were made in the fluorescence mode. Our analysis focuses on the film on MgO and uses the other two samples for comparison.

In contrast to the results of Stern *et al.* and Mustre de Leon *et al.*, the film data can be well described by a single, harmonic O(4) distribution that shows only very subtle changes near T_c. These data are very reproducible over a wide range of temperatures, and thus provide a null result to compare with any other results. On the other hand, the single-crystal data show a split O(4) distribution below T_c consistent with previous measurements on oriented powders. By comparing a case where the splitting is not present and one where it is, we show that previous XAFS measurements of a split O(4) distribution are not relying on an unusually small signal.

The measurements presented here also provide details of the harmonic broadening of the pair distribution of the atom pairs in the film on MgO. These measurements show interesting temperature dependences which are interpreted as changes in the correlations between the atomic positions in a given atom pair. Fluctuations in the broadening parameters of the Cu(2)-O(4) pair, and to a lesser degree in the Cu(1)-O(4) pair in the vicinity of T_c are also reported.

We begin our report by describing the experimental details in Sec. II. The data analysis procedures are given in Sec. III. The isolation of the O(4) contribution to the XAFS is presented in Sec. IV. Results of detailed fits to the film data are given in Sec. V. Consequences of observed features in the data are discussed in Sec. VI and the conclusions of this work are summarized in Sec. VII.

II. EXPERIMENTAL DETAILS

The thin-film samples of YBCO were deposited by off-axis single magnetron sputtering onto a MgO and a $LaAlO_3$ substrate. The film on MgO is estimated to be 5000-Å thick, and the film on $LaAlO_3$ is approximately 4000-Å thick. On cooldown, the films are brought into equilibrium with oxygen at 700 Torr at 450 °C. This condition fixes the chemical potential for oxygen. The maximum T_c occurs for the films when they are brought into equilibrium at 450 °C, 200 Torr of oxygen. This maximum is about 90 K. T_c drops somewhat for more oxygen (it drops about 1 K for annealing at 700 Torr) and for less oxygen. The maximum critical current at 4.2 K increases as the oxygen anneal pressure increases. This increase in the critical current is consistent with an increasing carrier density and a decreasing correlation length. Therefore the films are ''overdoped'' somewhat relative to maximum T_c.[21] The actual carrier concentration, and therefore the actual oxygen concentration, is not known since doping mechanisms other than oxygen incorporation exist, such as antisite disorder and substitions on the cation sites. The oxygen content is also affected by the large strains and high density of twin boundaries found in thin films.

X-ray-diffraction measurements indicate less than 1% impurity phases. The diffraction measurements also indicate that the films are oriented with their c axes perpendicular to the plane of the film with less than 1% a- or b-axis impurities for the film on MgO, and $<3\%$ for the film on $LaAlO_3$. TEM pictures confirmed that films created in the same way are c-axis oriented, with trace impurities and that the crystals are twinned. The transition temperatures were measured with the standard four-probe technique and found to be 89 K. A more detailed description of the sample preparation can be found in Ref. 22.

For comparison, we use a fairly large single crystal of YBCO which is nominally $YBa_2Cu_{2.958}Ni_{0.042}O_{6.95\pm0.005}$, that is, about 1.4% Ni substitutes for Cu. Although the oxygen content is well determined for this sample, the presence of nickel will affect the overall hole concentration and the local oxygen stoichiometry. Unlike other transition metals, Ni substitutes onto *both* the Cu(1) and the Cu(2) sites, and causes some distortions at least around the Cu(2) site.[23] Ni K-edge data from this sample are qualitatively consistent with our previous work on powders, but we could not further elucidate the nature of the distribution or the local distortions. Therefore we cannot know the local oxygen concentration around Cu sites and cannot say whether the local oxygen vacancies around the Cu(1) are the same or different than in $YBa_2Cu_3O_{6.95}$. The sample is, however, a high quality superconductor which is c-axis oriented with a $T_c=$ 89 K. Details of the sample preparation are described in Refs. 24 and 25. The thickness is estimated to be $\sim$ 17

μm by looking at the Cu K-edge step in the x-ray transmission spectrum.

X-ray fluorescence measurements were made on beamline 7-3 at the Stanford Synchrotron Radiation Laboratory. The samples were placed in an Oxford helium cryostat and oriented such that the incident x-ray beam was striking the surface of the samples between 10–12°. The x-ray-absorption cross section is proportional to $\langle \vec{\epsilon} \cdot \hat{r} \rangle^2$, where $\vec{\epsilon}$ is the polarization vector of the incoming light, and $\hat{r}$ is the unit vector pointing along the direction of the ejected electron. The amount of signal from atoms in the ab plane, such as the O(1) or O(2) oxygens, is small, since this plane is nearly perpendicular to $\vec{\epsilon}$; in this case, such a signal is $\sim \cos^2(79°) \cong 4\%$ of the signal from atoms along $\vec{\epsilon}$. Such a small signal cannot explain any of the effects we report in this paper.

Temperature was regulated via two sensors, one in the helium chamber and one about two inches above the sample. Because of the geometry and later calibration measurements, we estimate that the absolute temperature of the sample is probably 1–3 K higher than the sample sensor was indicating (the ''nominal'' temperature). Relative changes in the temperature of these data should be much better and is probably around 0.5 K. All reported temperature measurements of the XAFS data are the nominal temperature.

The fluorescence x rays from the film sample on MgO and the single crystal were detected using a 13-element Ge detector. This detector allows for energy resolution that isolates the Cu $K\alpha$ peak and eliminates any need for background fluorescences to be removed from these data. Count rates in each channel were kept well below saturation levels ($<$20% of saturation), but were in any case corrected for the dead-time-constant ($\sim$5–10 μs) introduced by the energy-resolving peak-shaping filters. Besides the ability to resolve the Cu $K\alpha$ fluorescence, the main utility in using the Ge detector is to aid in the removal of Bragg peaks in the absorption spectrum. Because the Bragg spikes occur at the incident beam energy, the energy resolving power of the Ge detectors can partially discriminate against them. However, a large change in the fluorescence flux can bring the detectors much closer to saturation, and thus the dead-time correction becomes more important. If a Bragg spike is particularly strong, the dead-time correction cannot account for the additional flux accurately enough, and the affected data must be removed. Such removal is accomplished by replacing the affected data by the normalized mean of the other channels. In this way we can usually generate a full absorption spectrum over the energies of interest with almost no experimentally induced spikes or dips. This method provides a significant advantage over more traditional single channel ionization counters when one realizes that for thin films on well-oriented substrates, or for single crystals, Bragg spikes can affect data over tens of eV.

Unfortunately, features which we call ''glitches'' can still arise from nonuniformities in the sample coupling to nonuniformities in the incident beam.[26,27] Since these occur in all the channels of the Ge detector, we must remove such features by fitting a low (second or third) order polynomial through neighboring (unaffected) data points and replacing these data with the fit. Fortunately, glitches often only affect between one and four successive data points, and so this procedure does not significantly alter the XAFS.

The fluorescence x rays from the YBCO film on $LaAlO_3$ were collected using a gas-ionization detector with a Ni filter. This detector does not allow for easy energy discrimination, and consequently background fluorescence from atoms other than the Cu atoms in our sample contribute $\sim$1/3 of the total x rays. This system allows us to look at some features of the XAFS spectrum from this sample, but does not allow for detailed fits to be performed with any reliability since amplitude information requires at least knowing the details of the background fluorescences, if not removing them (as with the Ge detector).

III. DATA ANALYSIS

Our data analysis procedures have been detailed elsewhere for standard transmission experiments. In this work, we will describe briefly the general procedure and only give details where significant differences in the procedure arise over Refs. 28–30.

A. Basic XAFS

The main features in an x-ray-absorption spectrum are due to single-electron excitations, namely, the photoelectric effect. These excitations appear as sudden jumps in the absorption coefficient $\mu(E)$. In a solid, the data just above these jumps exhibit oscillatory structure which has been named the x-ray absorption fine structure (XAFS). The XAFS are isolated by defining a function

$$\chi(E) \equiv \frac{\mu(E) - \mu_0(E)}{\mu_0(E)} \tag{1}$$

which is used just beyond the edge, normally $>$25 eV. $\mu_0(E)$ is a normalization function which is the absorption due to all processes that do not include the photoelectron backscattering effect described presently.

The oscillations in $\mu(E)$ are primarily due to an interference effect between the outgoing photoelectron's wave function and the part of the photoelectron's wave function which has scattered off nearby neighbors and returned to the absorbing atom. As the photoelectron's wave vector is increased, the interference is modulated with a frequency given by twice the distance to the backscattering atom. There are several other factors which must be taken into account. The version of the ''XAFS equation'' that we use in our data analysis is

$$\chi(k) = \mathrm{Im} \sum_i A_i \int_0^\infty \frac{g_i(r) e^{i[2r + 2\delta_c(k) + \delta_i(k)]}}{r^2} dr, \tag{2}$$

where the amplitude factor A_i is given by

$$A_i = N_i S_0^2 F_i(k), \tag{3}$$

N_i is the number of equivalent atoms in shell i, S_0^2 is the ''amplitude reduction factor'' that accounts primarily for many-body effects that reduce the XAFS oscillation amplitude such as shakeup or shakeoff, $F_i(k)$ is the backscattering amplitude of the photoelectron off neighbors i including a reduction due to the mean-free path of the photoelectron,

$g_i(r)$ is the pair-distribution function for the absorbing and backscattering atoms, and the phase shifts of the photoelectron from the central and the backscattering atom are given by $\delta_c(k)$ and $\delta_i(k)$, respectively. The distribution function $g_i(r)$ is usually taken to be harmonic:

$$g_i(r)=\frac{1}{\sqrt{2\pi}\sigma_i}e^{-(r-R_i)^2/2\sigma_i^2}, \tag{4}$$

where R_i is the average distance between the central and the backscattering atoms i, and the broadening factor σ_i (otherwise known as the Debye-Waller factor) combines the effects of thermal and static disorder. If a shell i contains atoms that are inequivalent, then σ_i may also be used as a measure of any distortion in the shell, even though such distortions are rarely harmonic.

In studies of well-ordered materials (such as YBCO) we expect there to be very little difference in the bond lengths measured by XAFS compared to diffraction. In fact, with the exception of the O(4) site, there are many XAFS studies which demonstrate the strong agreement between local structure in YBCO (and most of its relatives) and the average structure.[31–33] On the other hand, comparative measurements of the correlated Debye-Waller factors given by XAFS and the uncorrelated ones given by diffraction have been virtually ignored by most experimenters.

Part of the reason for not making direct comparisons between XAFS and diffraction broadening factors is that getting the absolute broadening factor is not always possible. Experimental measurements of amplitude functions have their own (usually unknown) broadening, and until recently, theoretical calculations were not of high enough quality to give reliable results. FEFF6,[34,35] written by Rehr and coworkers, has been shown to calculate accurate backscattering amplitudes and phase shifts, and even gives reasonable values for Debye-Waller parameters for simple materials with known Debye temperatures.[29,36] Such calculations provide a backscattering amplitude function with a known (zero) width for absolute comparison to real atom pairs. Although only experience will allow us to determine how accurate absolute measurements of correlated broadening factors really are, our limited experience indicates that they are probably within 10% in most cases.

Another reason direct comparisons are rarely made is simply that diffraction and XAFS width parameters measure different quantities. (A useful text describing more details beyond the following discussion is Ref. 37.) Diffraction relies on coherent diffracting of x-rays off many crystal lattice planes to generate a diffraction spot, and therefore its measurements of atom positions and broadening factors gives an average over many unit cells. XAFS depends only on the instantaneous (within $\sim 10^{-15}$ s) position of neighboring atoms with respect to the central (absorbing) atom, and therefore the broadening factors are a measure of variations in an atom-pair's distance. For example, if two neighboring atoms are vibrating with the same (spatial) amplitude W but are somehow rigidly connected, the bond length would never change, and XAFS would measure a zero width. Diffraction would measure broadening factors for the two atoms to be W. Mathematically, if δr_X is the instantaneous deviation of atom X's position from its mean position, the average deviation in the distance between atoms A and B is given by

$$\sigma_{AB}=\sqrt{\langle(\delta r_A-\delta r_B)^2\rangle}=\sqrt{\langle\delta r_A^2\rangle+\langle\delta r_B^2\rangle-2\langle\delta r_A\delta r_B\rangle}. \tag{5}$$

If we define $\sigma_A=\sqrt{\langle\delta r_A^2\rangle}$ (which equals $\sqrt{U}$ in conventional diffraction notation), then the last term can vary between $-2\sigma_A\sigma_B$ and $+2\sigma_A\sigma_B$, depending on the degree to which the motions of the two atoms are correlated. One can define a ''correlation'' parameter ϕ from

$$\sigma_{AB}^2=\sigma_A^2+\sigma_B^2-2\sigma_A\sigma_B\phi. \tag{6}$$

Since σ_A^2 is given by diffraction experiments, we can provide measurements of correlation factors. ϕ will vary between $+1$ for atoms vibrating in phase with each other (like in an acoustical phonon), 0 for atom pairs that are separated by a few unit cells at temperatures well above the Debye temperature, and -1 for pairs that are moving out-of-phase with each other (like in an optical phonon). Of course since the XAFS measurements give average atom-pair distances over the crystal, static disorder can produce the same results. These concepts assume Gaussian forms for the distribution functions. If anharmonic distributions exist, the interpretation of measurements of ϕ will be more ambiguous.

B. Data reduction

An initial estimate of $\chi(k)$ is obtained by approximating $\mu_0(E)$ in Eq. (1) by a cubic spline though $\mu(E)$, k by $\sqrt{2m(E-E_0)}/\hbar$ and E_0 by the energy at the half height of the edge. The data are fit in r space as described in Ref. 28. The fit is then subtracted from the data to obtain a residue which can be utilized to make a better estimate for $\mu_0(E)$, as described in Ref. 30.

The data have been corrected for the additional ''self-absorption'' of the fluorescing photon in the sample using a treatment which goes slightly beyond the usual correction (for instance, see Tröger *et al.*[38]) by including the finite thickness of the sample and the effect of the XAFS oscillations in the correction term. This amplitude correction for the 5000-Å film is small [$\sim 8\%$ of $\chi(k)$], but for the 17-μm single crystal the correction is more significant [$\sim$ 60% of $\chi(k)$].

An example of $k^3\chi(k)$ for the film on MgO which has been obtained using the above procedures is displayed in Fig. 1. The Fourier transforms (FT) of $k^3\chi(k)$ for these data as well as for one temperature of the single-crystal data are shown in Fig. 2.

IV. ISOLATING THE XAFS SIGNAL DUE TO THE O(4) CONTRIBUTION

Since the information above 2.5 Å is complicated, we had to perform fits to the data to discern any information about the Y, Ba, and Cu environment. These fits are described in Sec. V. However, since the Cu(1)-O(4) and Cu(2)-O(4) peaks are relatively well separated, we can isolate them and back transform the data to k space. Mustre de Leon *et al.* based their argument on the fact that the O(4) position was split by observing anharmonic behavior in the Fourier-

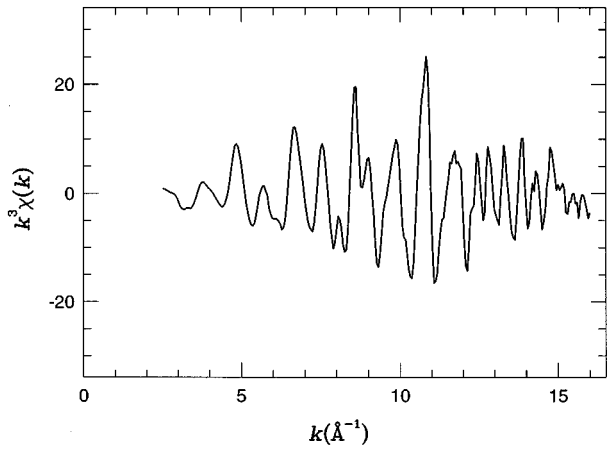

FIG. 1. $k^3\chi(k)$ vs k for a YBCO film on MgO at $T=20$ K with the x-ray polarization parallel to the c axis of the film. These data have been dead-time corrected and had some minor glitches removed, as described in the text. Data from the single crystal are of comparable quality. Data from the film on $LaAlO_3$ have similar signal-to-noise, however, the energy range is shorter.

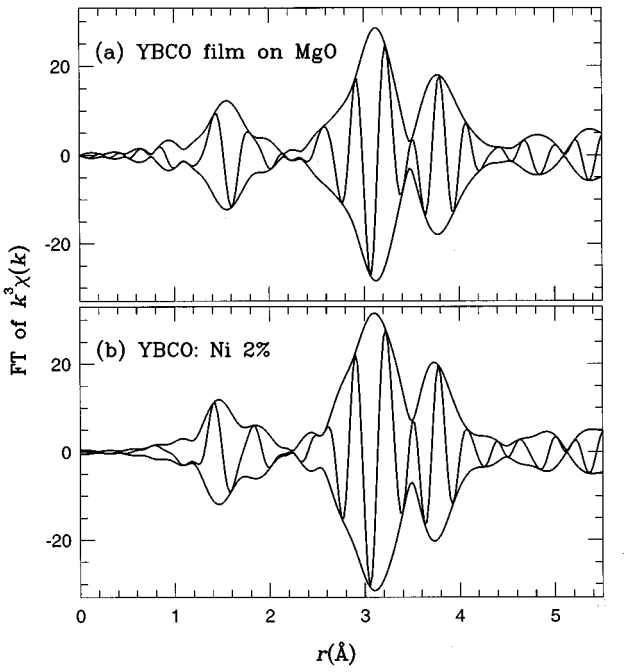

FIG. 2. The Fourier transform (FT) of $k^3\chi(k)$ $[\equiv\tilde{\chi}^3(r)]$ vs r for (a) the same sample as in Fig. 1, and (b) the single crystal of YBCO: Ni 1.4%. Data are transformed with a Gaussian window between 3–15.5 Å^{-1} and broadened by an additional 0.3 Å^{-1}. The oscillating curve is the $\text{Re}(\tilde{\chi}^3)$, and the envelope of this curve is the amplitude, $[\text{Im}(\tilde{\chi}^3(r))^2+\text{Re}(\tilde{\chi}^3(r))^2]^{1/2}$. The peak at 1.55 Å corresponds to the Cu(1)-O(4) atom pair, while the shoulder of this peak at 2.0 Å corresponds to the Cu(2)-O(4) atom pair. The multipeak between 2.4 and 3.4 Å is a combination of the Cu(2)-Y, Cu(2)-Cu(2), Cu-Ba, and Cu(2)-O(2,3) atom pairs. Lastly, the peak at 3.8 Å is the Cu(1)-O(4)-Cu(2) multiple-scattering peak. The peak positions are shifted from the actual pair distances because of the combined effect of δ_c, δ_i and $F_i(k)$ in Eq. (2).

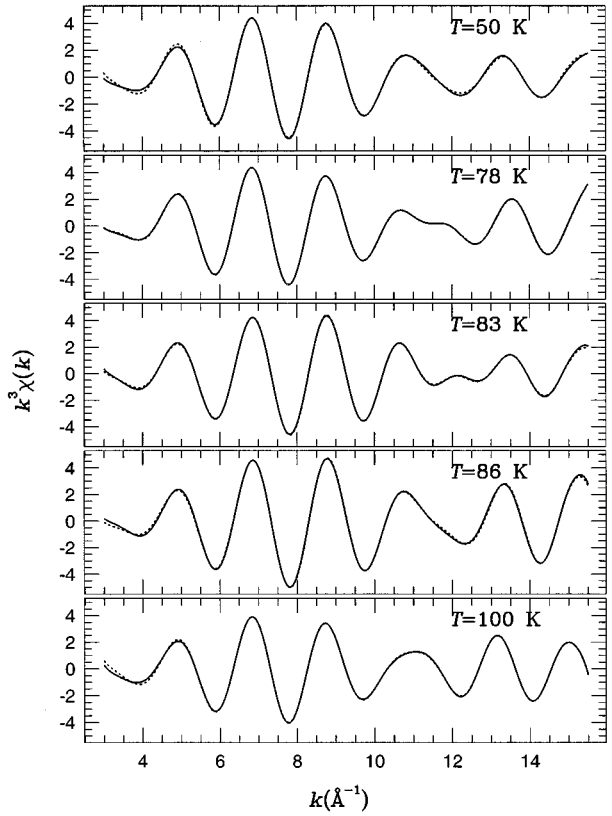

FIG. 3. O(4) contribution to $k^3\chi(k)$ vs k at several temperatures for the single crystal of YBCO: Ni 1.4%. The solid lines are the data and the dotted lines are the fits. Each fit assumes a split O(4) site except the $T=100$ K fit. The O(4) contribution was obtained by back transforming r-space data (Fig. 2) between 1.3–2.2 Å. Contributions from higher shells [say, from the Cu(2)-Y peak] have been shown to be negligible (Ref. 6).

filtered k-space data in the form of a beat near 12 Å^{-1}. If a two-site distribution exists, we expect the contributions of the two atom pairs to be split into four distinct distances: two corresponding to the mean Cu(1)-O(4) distance $\pm$ the splitting ($R_{\text{Cu}(1)-\text{O}(4)}\pm\Delta_r/2$) and two corresponding to the mean Cu(2)-O(4) distance $\pm$ the splitting ($R_{\text{Cu}(2)-\text{O}(4)}\pm\Delta_r/2$). Since the XAFS signal for each of these distances is oscillatory, a small splitting will generate a beat in the XAFS signal at a k vector given by $2k\Delta_r=\pi$. In order to make our data directly comparable to their's, we have also isolated the O(4) contribution in this way. First, the FT of $k^3\chi(k)$ was obtained as in Fig. 2. We chose k^3 weighting for this transform because the O(4) peak is much better resolved than in a k-weighted transform. The Fourier transforms of the $k^3\chi(k)$ data were then back transformed from 1.3 to 2.2 Å. The O(4) contribution from this procedure is displayed for the single crystal in Fig. 3 and for the film on MgO in Fig. 4. The sinusoidal behavior in both these figures is the sum of the Cu(1)-O(4) and the Cu(2)-O(4) components.

The O(4) contribution in the single crystal displayed in Fig. 3 is in rough agreement with the original work of Mustre de Leon;[5] although the data in the 11–13 Å^{-1} range varies from temperature to temperature, the $T=83$ and 86 K data show clearly anharmonic behavior near 12 Å^{-1}, indicating a splitting of about $\Delta_r\simeq 0.13$ Å. In fact, except for the

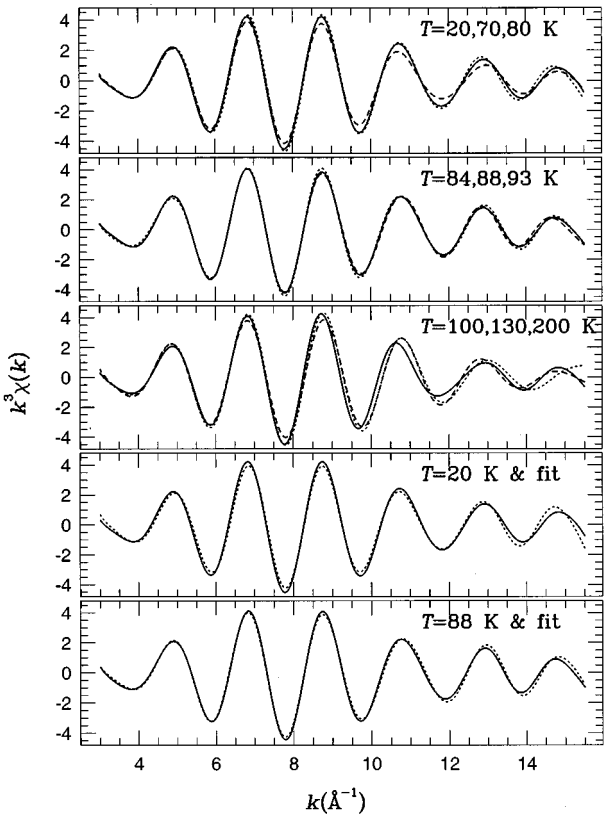

FIG. 4. O(4) contribution to $k^3\chi(k)$ vs k at several temperatures for the YBCO film on MgO. The O(4) contribution was obtained in an identical fashion to the data in Fig. 3. Only half the data are displayed for clarity; an additional scan was taken in between each of the temperatures displayed here. The bottom two panels show fits to the O(4) contribution to $k^3\chi(k)$ vs k for the YBCO film on MgO at $T=20$ and 88 K. Fits assume a single O(4) site.

$T=100$ K data, none of the single-crystal data can be fit with a single, harmonic distribution for the O(4) site (Sec. V B).

The data from the film on MgO in Fig. 4, on the other hand, displays harmonic behavior at all temperatures and shows very little change from temperature to temperature. This harmonic behavior persists out to 16 Å^{-1}. Since a beat may still occur at higher wave vectors, these Fourier-filtered k-space data set an immediate upper limit of 0.10 Å. The character of the film data is distinctly different than the single crystal data, showing little if any splitting. This result also applies to the film on $LaAlO_3$ (Fig. 5) and therefore may be a generic result of YBCO films. However, it should be noted that this film was grown under similar conditions to the film on MgO.

V. FITS

Although the raw data has provided much useful information about the nature of the O(4) site distribution, we can still learn more details both about the O(4) distribution and about the further neighbors by performing fits of the spectra to the sum of theoretical standards. Such fits provide more quantitative details about the local environment around the copper atoms and allow us to deconvolve the contributions of overlapping peaks due to the Cu(2)-Y, Cu(2)-Cu(2) (between the planes), Cu(2)-Ba, Cu(1)-Ba and the Cu(1)-Cu(2) pairs. Furthermore, by fitting the data to theoretical standards calculated by FEFF6 we can obtain absolute estimates of the broadening factors σ and compare them to results from diffraction studies, thus allowing for measurements of the correlation parameter ϕ [Eq. (6)]. We only report fit results beyond the near-neighbor Cu(1)-O(4) and the Cu(2)-O(4) atom pairs as a function of temperature for the YBCO film on MgO data.

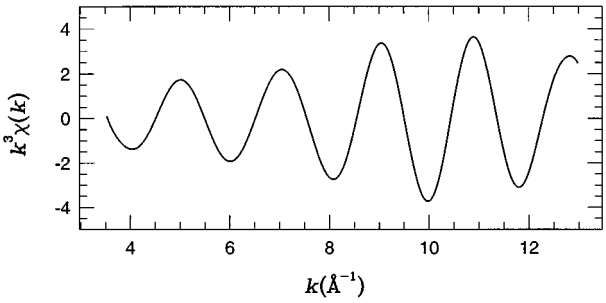

FIG. 5. O(4) contribution to $k^3\chi(k)$ vs k for the YBCO film on $LaAlO_3$ at $T=70$ K. Full spectrum $k^3\chi(k)$ data were transformed between 3.5–13 Å^{-1} (Gaussian broadened by 0.3 Å^{-1}), and then back transformed between 1.4–2.2 Å. The range of data does not extend to as high k as the data in Figs. 3 and 4, however, there is no beat feature in the 11–12 Å^{-1} region in contrast to the data in Fig. 3.

A. Fitting procedures

Although weighting the XAFS $\chi(k)$ by a factor of k^3 enhances the high k data where the beat in the O(4) part of the spectrum is likely to occur, we have found that fits to data weighted by a single factor of k give more reliable results overall. In general, if we are not focusing on the O(4) part of the spectrum, we fit our data to the FT of $k\chi(k)$. Fitting to the FT reduces the effect of overlapping peaks.[28] Since XAFS can be thought of as a sum of the contribution to the absorption of the individual atom pairs, we calculate $F(k)$, $\lambda(k)$, $\delta_c(k)$, and $\delta_i(k)$ given an approximate atom cluster for each scattering path using FEFF6. This information for each path is called a ''standard.'' The data are fit to a sum of theoretically calculated standards which include all single-scattering paths up to the Cu(1)-Cu(2). The only multiple-scattering paths that are included involve the Cu(1)-Cu(2) path and the intermediate O(4). The Cu(2)-planar oxygen path across the planes (~3.65 Å) was too low in amplitude to obtain reliable fit results, so its parameters were fixed. Other multiple-scattering paths were found to be negligible, or were dominanted by the single-scattering paths.

Several of the parameters were constrained in order to decrease the number of fit parameters. The Cu(2)-Y and the Cu(2)-Cu(2) distances were constrained such that the yttrium rests in the center of the eight Cu(2) neighbors given the diffraction measurements of the a and b lattice parameters of typical samples. This constraint was necessary to fit the Cu(2)-Cu(2) peak (3.38 Å), which is small compared to the nearby Cu(2)-Y (3.21 Å), Cu(2)-Ba (3.37 Å), and Cu(1)-Ba peak (3.48 Å). Also, if the Cu-Ba peaks were allowed to vary

over a broad range, they would often fall into a false minimum in the fitting parameter such that they were ~ 0.04 Å too long. This behavior was noted by Stern *et al.*[9] However, we were able to determine by fits to CuI data (a Cu-I standard should be very similar to a Cu-Ba one) that this error was due primarily to the overlap of several neighboring peaks in YBCO, and not to unusual errors in the FEFF6-generated backscattering amplitude. We therefore only allowed the Cu-Ba peaks to vary over a narrow range (± 0.02 Å from the diffraction result). All width parameters were allowed to vary freely, except $\sigma_{\mathrm{Cu(2)-O(2,3)}}$ (across the planes), which was held fixed. E_0's for like atoms were held equal, but were allowed to vary between different types of atoms to help correct for minor errors in the FEFF6 phase calculations.

The aim of these fits is to identify parameters that change with temperature. Since measurements of S_0^2 and σ are correlated, we performed a fit where these parameters were allowed to vary freely, and then calculated the average for S_0^2 for each peak. A similar correlation occurs between measurements of R_i and E_0, so average E_0's for the individual peaks were also determined. The values of S_0^2 and E_0 were then fixed for each path and the fits were performed again. By holding S_0^2 and E_0 fixed for all temperatures, we ascribe all changes in the peaks' amplitude and frequency with temperature to changes in σ_i and R.

Although S_0^2 should be the same for all paths in principle, we found that if a single value of S_0^2 was used high-quality fits could not be obtained for the Cu(1)-Cu(2) peak [which includes multiple scattering off the O(4) atom]. The fit was improved by allowing this one peak to have an $S_0^2=0.75$, while all other peaks use an $S_0^2=0.90$.

The maximum number of parameters given our fit range using the method of Stern[39] is 29. The total number of parameters in these fits was 17, well below the maximum.

Errors in the parameter measurements are difficult to estimate reliably in XAFS fits. We estimate the errors on all the parameters from the covariance matrix generated by the fit. The variance of the data used in the covariance matrix is obtained by assuming that the residual difference between the data and the fit is normally distributed. This procedure only accounts for random errors and thus should describe relative errors between data at nearby temperatures. Systematic errors due to problems in the FEFF6 calculation, self-absorption corrections, estimates of μ_0, etc., will cause overall shifts in the best fit. Absolute errors on these measurements are roughly $\lesssim \pm 0.01$ Å in R and $\lesssim \pm 10\%$ in S_0^2 and σ for the near-neighbor oxygens,[29] and $\lesssim \pm 0.02$ Å in R and $\lesssim \pm 15\%$ in S_0^2 and σ for the overlapping neighbors between 3 and 4.1 Å.

B. Fitting results

1. O(4)-site distribution in the single crystal

As suggested by the presence of the beats, a two O(4)-site distribution was necessary to fit the single-crystal data in Fig. 3 for the four lowest temperatures. The fits shown in Fig. 3 all assume a two-site distribution for the O(4) except for the $T=100$ K data. For the $T=100$ K data, a single site for the O(4) produces a reasonable fit; the slight dip in the amplitude at ~ 11 Å^{-1} can be modeled by an interference between a single Cu(1)-O(4) path and a single Cu(2)-O(4) path. Note that the data in this region are still visibly different from the film data. The features in the $T=50$, 78, 83, and 86 K data between 10 and 13 Å^{-1} are modeled by two Cu(1)-O(4) paths and two Cu(2)-O(4) paths, with each path length split by 0.12 ± 0.01 Å and 0.06 ± 0.06 Å, respectively. We did not observe any obvious trend with temperature other than for the $T=100$ K data.

The two-site fits to the single-crystal data may be deceptively good. In order to obtain these fits, unphysically small (<0.01 Å) values for the broadening factors were needed. In addition, the sum of the amplitudes for these peaks (which should add up to the number of neighbors times S_0^2) is about 50% too high. These exceptionally narrow peaks indicate that besides the split peak distribution, further anharmonicity must exist. A common way to model anharmonicity in XAFS data analysis is to expand Eq. (2) about R_i for a given atom pair in powers of $\langle r^n\rangle$, otherwise known as a ''cumulant expansion'' ($\langle r^n\rangle$ is the nth moment, M_4 is the part of the fourth moment that is different from a Gaussian, namely $M_4=\langle r^4\rangle-3\sigma^4$).[40] The second cumulant is the width in the harmonic approximation, or the Debye-Waller factor. The third cumulant affects the phase shift. The fourth cumulant multiplies the overall amplitude by a factor $e^{(2/3)k^4M_4}$. If the exponent in this term is positive, it *increases* the amplitude of the XAFS at higher wave vectors, acting like an imaginary Debye-Waller factor, or like a distribution with a cusp which takes weight from the center of the distribution and puts it into the wings.[41] Excellent fits to the single-crystal data can be obtained by allowing the four Cu-O(4) peaks to have $M_4\cong 2.7\times 10^{-5}$ Å^4. These fits have much more reasonable Debye-Waller factors (~ 0.04 Å) and S_0^2 is no longer 50% too large. With such a large value of M_4, the cumulant expansion is no longer accurate above a k of ~ 14 Å.

These fits serve to illustrate that we can model the O(4) site distribution with reasonable values for the fit parameters, but that the fits are not unique. Because S_0^2, σ, and M_4 are so correlated for these slightly separated Cu-O(4) peaks, a study of the temperature dependence of any of these parameters would produce questionable results. The only firm result is that at least three, and possibly four, atom-pair distances are necessary to describe the beat structure in the k-space transforms for the single crystal. The actual O(4)-site distribution $g(r)$ may be more complicated. Table I reports fit results to the further neighbors for the $T=50$ K sample.

2. Fits to the film on MgO

The Cu(1)-O(4) and Cu(2)-O(4) peaks are well fit by a single O(4) site in the film data (Fig. 4), as suggested in Sec. IV. Allowing for a two-site distribution with a $\Delta_r\gtrsim 0.09$ Å did not produce reasonable fits. Fits to the film data of a similar quality as to the single-crystal data are obtained without assuming any anharmonic behavior in the atom-pair distances out to ~ 4.1 Å. Figure 6 shows the fit to the film data over this range both in k space and in r space, and Table I reports the fit to all the parameters for both the single crystal and the film on MgO at $T=50$ K. No significant deviation between the XAFS atom-pair distance measurements and standard diffraction measurements were observed, except for

TABLE I. Comparison between fit results to the single crystal of YBCO:Ni 1.4% (xtal) and the film of YBCO on MgO at $T=50$ K. *n.b.* stands for ''number of bonds per unit cell.'' Neutron-diffraction results of Sharma *et al.* (Ref. 43) are also given for comparison, and measurements of ϕ are reported for the film data. Errors marked with an ''×'' are unreliable because the pair-distribution function deviates significantly from a Gaussian. Imaginary Debye-Waller factors often accompany these distributions; such parameters cause the XAFS oscillations to *increase* with k. Some parameters were held fixed or constrained in the fits. See Sec. V B for further discussion.

	XAFS xtal			XAFS film			Neutron Diff. (Ref. 43)				Film
Bond	r (Å)	*n.b.*	σ (Å)	r (Å)	*n.b.*	σ (Å)	r (Å)	*n.b.*	σ_A (Å)	σ_B (Å)	ϕ
Cu(1)-O(4)	1.833(4)	1	i0.04(×)	1.861(2)	2	0.035(2)	1.8588(13)	2	0.047(16)	0.064(9)	0.85(5)
Cu(1)-O(4)$_b$	1.941(4)	1	i0.01(×)		0			0			
Cu(2)-O(4)	2.220(5)	1	0.04(×)	2.264(3)	2	0.059(2)	2.2684(15)	2	0.037(14)	0.064(9)	0.6(1)
Cu(2)-O(4)$_b$	2.337(5)	1	i0.01(×)		0			0			
Cu(2)-Y	3.182(7)	8	0.029(6)	3.191(8)	8	0.039(4)	3.2041(5)	8	0.037(14)	0.034(16)	0.44(10)
Cu(2)-Cu(2)	3.349(8)	8	0.10(2)	3.358(8)	8	0.19(6)	3.386(1)	8	0.037(14)	0.037(14)	-3(2)
Cu(2)-Ba	3.382(15)	8	0.024(8)	3.38(1)	8	0.037(8)	3.367(1)	8	0.037(14)	0.046(16)	0.60(8)
Cu(1)-Ba	3.475(8)	8	0.027(9)	3.472(4)	8	0.037(8)	3.462(1)	8	0.047(16)	0.046(16)	0.55(11)
Cu(2)-O(2,3)	3.65(2)	2	0.12(1)	3.656(3)	2	0.12(4)	3.6583(5)	2	0.037(14)	0.056(17)	-2(3)
Cu(1)-Cu(2)	4.102(5)	2	0.058(1)	4.106(4)	2	0.064(1)	4.1272(1)	2	0.047(16)	0.037(14)	-0.03(10)

the unusually short Cu(2)-O(4), Cu(2)-Cu(2), and Cu(1)-Cu(2) pairs, which are about 0.02 Å shorter than in the single-crystal diffraction measurements. Although the c-axis lattice parameter was not measured from diffraction experiments on these samples, samples made under similar conditions have c-axis lattice parameters between 11.68 and 11.72 Å. Therefore, the short atom pairs measured by XAFS indicate some systematic error, either in the model or in the standards. In particular, these differences could be related to systematic errors in FEFF6-generated standards that occur in the wings of the backscattering amplitude in r space.[29] Both the Cu(2)-O(4) and the Cu(2)-Cu(2) signals are small compared to the other peaks in the spectrum, and therefore are more susceptable to the wings of the Cu(1)-O(4), Cu-Ba, and Cu-Y signals. The Cu(1)-Cu(2) peak has a large signal; however, the standard also involves the intervening O(4) atom, in addition to having significant overlap of its backscattering function with the Cu-Ba pairs.

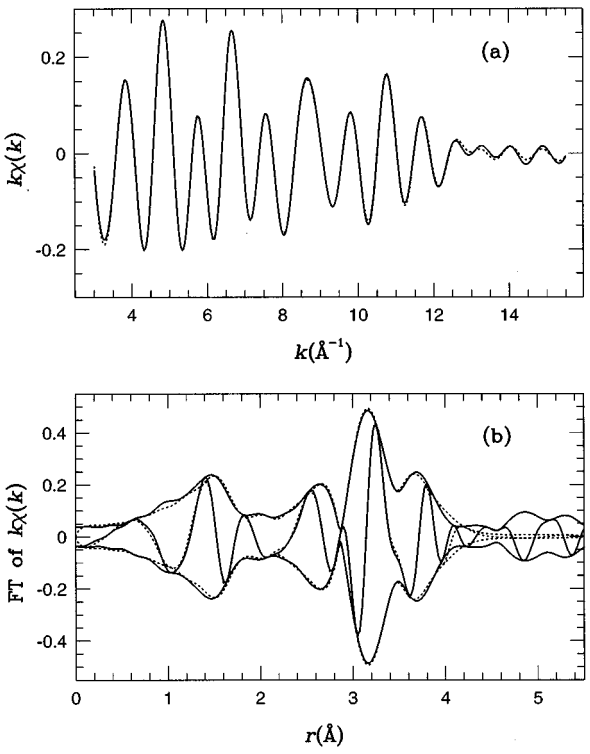

FIG. 6. Full fit to (a) $k\chi(k)$ vs k and (b) FT of $k\chi(k)$ vs r for the YBCO film on MgO. Data in (a) are the back transform of the data in (b) from 1.3–4.0 Å in r space. The FT range in (b) is the same as in Fig. 2. Notice that the quality of the fit is very good at low k and degraded somewhat at high k.

Plots of σ vs T are shown in Fig. 7. All the atom pairs show an increase of σ with temperature, except the Cu(1)-O(4) and the Cu(2)-Cu(2) (not shown) atom pairs. The measurements of $\sigma_{\text{Cu(2)}-\text{Cu(2)}}$ are fairly large ($\sim$0.11 Å) with large estimated errors and are therefore unreliable. Only the Cu(1)-O(4) and the Cu(2)-O(4) pairs show any anomalies in σ near T_c. σ for both pairs increases slightly just above T_c and then returns just below T_c. The jump is larger for the Cu(2)-O(4) width ($\sim$0.008 Å) than for the Cu(1)-O(4) width ($\sim$ 0.004 Å). This behavior was noted for the Cu(1)-O(4) bond both by Stern *et al.*[9] and Kimura *et al.*,[42] although the Stern result assumed a split O(4) site. None of the previous XAFS studies report a change in the Cu(2)-O(4) width. All other atom-pair parameters show smooth behavior with temperature and are of reasonable values.

C. Correlations of the further neighbors

We have analyzed the correlations between positions of the Cu atoms and their near neighbors by calculating ϕ for each atom pair. Diffraction measurements of broadening factors for each site are required, as indicated in Eq. (6). We have chosen temperature-dependent neutron-diffraction data given by Sharma *et al.*[43] because they include a relatively dense grid in temperature between data points ($\Delta T \cong 10$ K), measurements over a similar range of temperatures (10–300 K) to this study, anisotropic thermal factors for the O(4) site, and a high sensitivity to the oxygen atoms. This diffraction study saw no anomalous features with temperature in the thermal factors for any lattice site and is consistent with a

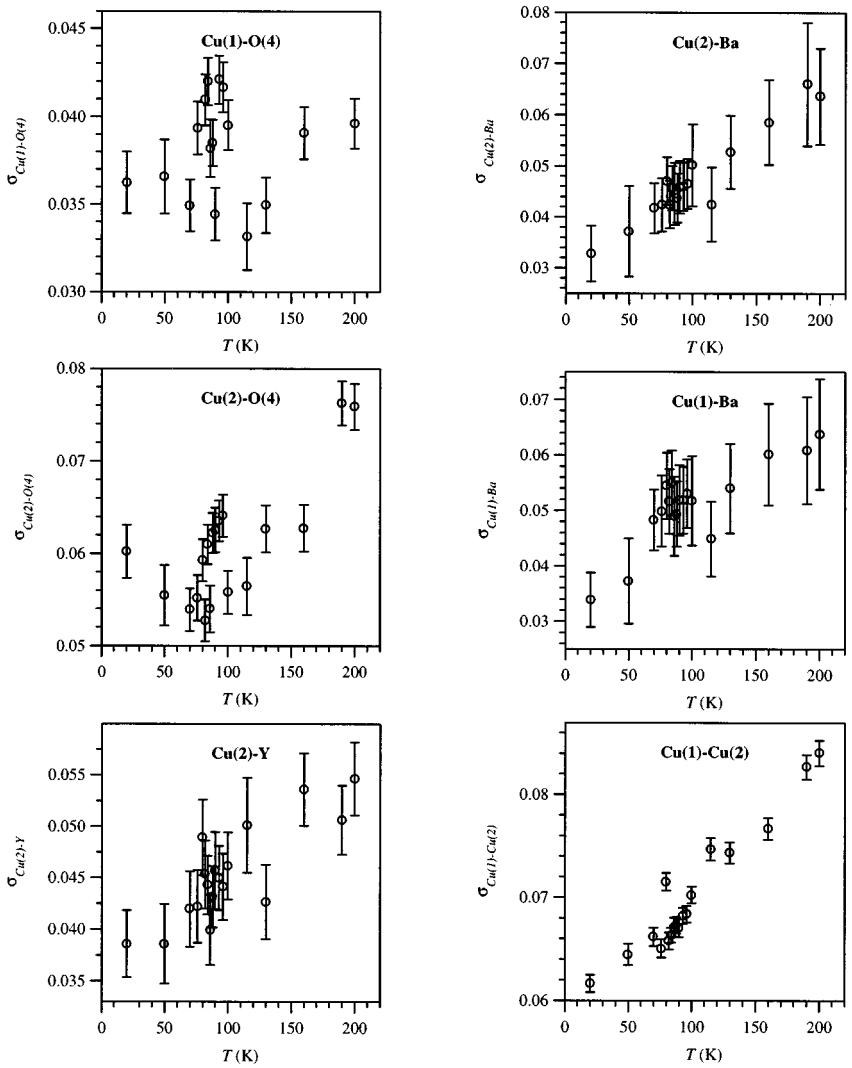

FIG. 7. σ vs temperature from the film of YBCO on MgO for all single-scattering paths up to 4.15 Å, except the Cu(2)-Cu(2) (at ~3.38 Å) and the Cu(2)-O(2,3) (at ~3.66 Å) pairs. Errors are estimated from the covariance matrix, and in no way reflect any systematic errors, as discussed in Sec. V A. These errors should thus be taken as relative errors which indicate the reproducibility of the data.

similar study by Kwei *et al.*[44] Since the measurements of Sharma *et al.* of the thermal factors were not always at the same temperatures as the measurements in this report, we fit each Debye-Waller factor from diffraction vs temperature with a polynomial. The use of these thermal factors may introduce systematic errors into our measurements of ϕ not only because the samples are prepared with different methods in different laboratories, but also because the diffraction results were obtained from a powder of YBCO and our data is for a film. Unfortunately, we must tolerate such errors because no comprehensive, temperature-dependent study of a thin film of YBCO exists at this time. Such errors should only contribute to an overall shift of the ϕ parameter and should not greatly affect the temperature dependence unless major features in the (as yet, unmeasured) diffraction thermal factors occur in measurements on films and not on single crystals.

The correlation coefficients vs temperature for each atom pair are displayed in Fig. 8. Errors are propagated from the quoted errors in Ref. 43 and the errors in Fig. 7 and in no way attempt to reflect any systematic errors introduced by FEFF6, differences in the samples, etc. The correlations for the Cu(2)-Cu(2) bond are not displayed because our measurements of $\sigma_{\mathrm{Cu}(2)-\mathrm{Cu}(2)}$ are unreliably large with large estimated errors. All the other atom pairs are resolved in the fits well enough to give reasonable estimates of ϕ.

VI. DISCUSSION

A. Split O(4) site

The main result reported above is that while two O(4) sites are necessary to describe the XAFS data for a single crystal very well, a high-quality fit to XAFS data for the thin film with a single O(4) site is also possible. Although this result only puts an upper limit on the size of any site splitting at $\lesssim$0.09 Å, the measurements of the Debye-Waller factors are small enough to indicate that any possible splitting is probably even smaller. (Any unresolved splitting should add to the thermal Debye-Waller factors in quadrature.)

Even though the existence of the splitting in some samples is now well established, the nature of the splitting is still quite unclear. The main problem is that the split sites could be due to motions of individual atoms between distinct sites, or due to two separate harmonic potentials, displaced from each other by, perhaps, a local distortion. One model[15] for static splitting relies on oxygen vacancy ordering on the O(1) site, which may shift the local position of the O(4)

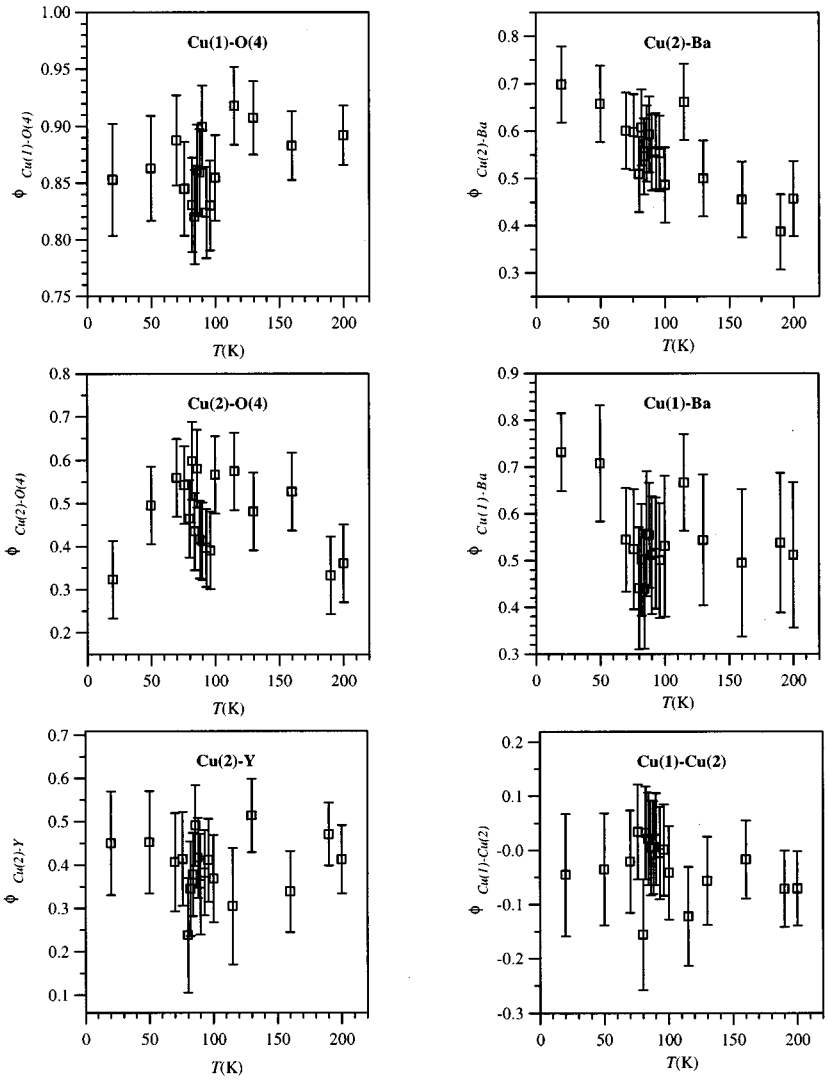

FIG. 8. The correlation coefficient ϕ vs temperature from the film of YBCO on MgO for the same atom pairs as in Fig. 7. Errors are propagated through Eq. 6 using the errors for the diffraction data reported in Ref. 43.

atom. At least one configuration of oxygen vacancies can produce a split O(4) position when half of the O(1) sites are occupied: the Ortho-II phase of $YBa_2Cu_3O_{6.5}$, which occurs when every other Cu-O(1) chain is completely vacant of oxygen. In this case, only half the O(4)'s have near O(1) neighbors. This configuration splits the O(4) site into two sites separated by ± 0.05 Å from the stoichiometric [no O(1) vacancies] site.[16,17] Röhler[15] considers a similar situation when single O(1) vacancies cause shifts in the O(4) position both along the same chain and along neighboring chains. In this model a single O(1) vacancy affects 12 O(4) atoms. In the case of YBCO with $\delta = 6.95$ (as in our single crystal), this would mean 60% of the O(4) oxygens could be affected. This model can also explain why the effect seems to be more easily fit as a split O(4) distribution in lower T_c samples [i.e., more O(1) vacancies] as measured by Stern *et al.*[9] Any changes observed in the splitting near T_c would be considered a reordering of oxygen vacancies in this model. In order to explain the thin-film results, one would have to consider that the oxygen concentration is similar in the film and the single crystal (Sec. II). Instead, one might invoke the added stress on the material introduced by the substrate. This stress could perhaps be manifest as a freezing of the vacancies into a random organization that suppresses the amount of splitting. This hypothesis is not likely, however, because oxygen diffusion measurements are not drastically different in a film compared to crystals.[45,46] Another possibility is that the films are overdoped and hence there are very few O(1) vacancies. Indeed, the films are overdoped with respect to T_c, however other factors may contribute to the actual number of oxygen vacancies, such as defects. A direct test of this argument would be to measure films that range from overdoped to very underdoped [i.e., many O(1) vacancies].

A dynamic model that would lead to either a broadening or a split O(4) position is the hopping small-polaron model, with the polaron hopping on and off the Cu-O(4) bonds as discussed by Mustre de Leon *et al.*[6] Ranninger[13] has calculated the XAFS signatures for the presence of polarons and shown that as the hopping speed decreases, the pair-distribution function first broadens and then splits; less than a factor of 2 in hopping speed is required to change from a broadened peak to a split peak. This is expected from the following simple argument. When the electron hops at a much faster rate than the lightest optical phonons, the lattice cannot respond, and there is little displacement of the individual atoms. If the hopping is slower, the lattice has time to respond, and the Cu and O(4) atoms move towards each other or apart as the polaron hops on and off the ligand. If

the hopping rate falls below the optical frequency, a split Cu-O(4) distribution emerges, corresponding to the absence or presence of the polaron. This model can easily explain both the single crystal and the thin-film results with a small change in the polaron hopping rate. The fact that the Cu(2)-O(4) peak is less ordered than the Cu(1)-O(4) peak and has a correlation parameter ~ 0.5 is consistent with such a model.

Although the oxygen vacancy argument has possible merit, there is a body of literature that links dynamics of the O(4) site to anomalies in vibrational spectroscopies both in YBCO (Refs. 10, 47, and 48) and other materials.[10,47,49,50] Since XAFS is not sensitive to static verses dynamic changes in atomic positions, there is little chance the XAFS technique can resolve this issue. However, XAFS can determine whether a pair-distribution function is harmonic or not. In our fits to the split distribution in the single crystal, we had to allow for a large fourth cumulant for both O(4) sites. This term can either have the effect of flattening out or sharpening the peak of an otherwise harmonic distribution, depending on the sign. These data required a positive fourth cumulant, and were thus sharper than a harmonic distribution. No third cumulant was necessary to fit the data. The necessity of this extra parameter indicates that the pair-distribution function is not simply the sum of two harmonic distributions. The need for this quartic term is consistent with Raman measurements of the O(4) mode at 505 cm^{-1} which also requires a significant fourth-order term.[10] This anharmonicity has been speculated[10] to be related to the anharmonic potential implied by the split O(4).[6,51] The anharmonicity in the O(4) 505 cm^{-1} mode could now be directly linked to the split O(4) distribution if accurate measurements of the Raman anharmonicity can be shown to be significantly different between a film and a single crystal. This result would mean that the anharmonicity (and any polaron formation related to this anharmonicity) is not required for high-T_c superconductivity. On the other hand, if the anharmonicity in the 505 cm^{-1} peak is unchanged between the film and the crystal, then the split O(4) is not related to it. In this scenario, polaron formation may still exist and be important for high-T_c, but the split O(4) would not be the structural manifestation of it.

When trying to explain why splitting of the O(4) site may or may not be present, one should also consider the T_c dependence. Stern *et al.* reports that the changes in the splitting near T_c are more pronounced for the lower T_c samples. However, the two-site fits to the O(4) for the higher T_c samples in their work are not of the same high quality as for the lower T_c samples. In other words, the pair-distribution function for these samples appears to be more complicated than a simple two-site distribution, so the Stern fits cannot really rule out any significant temperature dependence. In any case, for some samples, they report a constant splitting at all temperatures. This result is in contrast to the work by Mustre de Leon *et al.*, where they report the splitting to be constant at all temperatures, except near T_c where the splitting shrinks from 0.13 to <0.11 Å. The results of our work on the single crystal also indicate that the temperature dependence may not be consistent from sample to sample: all the data at $T<T_c$ cannot be fit satisfactorily with a single O(4) site, yet the $T=100$ K data are well described with a single O(4) site.

B. Changes in broadening parameters

In our measurements of the broadening parameters of the film on MgO we observe some significant temperature dependences. Almost all the measured bonds show the Debye-Waller factor increasing with temperature, as one expects if the Debye temperature is not too large (Fig. 7). The exception is the Cu(1)-O(4) bond which maintains a broadening of approximately 0.035–0.40 Å from $T=20$ to 200 K. The only significant behavior occurring near T_c involves the O(4) atom: both the Cu(1)-O(4) and the Cu(2)-O(4) pairs show an increase in their broadening parameter, with $\sigma_{\mathrm{Cu(1)-O(4)}}$ jumping from 0.035 to 0.040 between 80 and 100 K and back then to 0.035 Å, and $\sigma_{\mathrm{Cu(2)-O(4)}}$ jumping from 0.060 to 0.068 Å between 80 and 96 K and back to 0.060 Å. In the region between $T=80$ and 100 K, both $\sigma_{\mathrm{Cu(1)-O(4)}}$ and $\sigma_{\mathrm{Cu(2)-O(4)}}$ varies from temperature to temperature more than the estimated error. This fluctuation may be real or the error estimates may be too small for some reason, perhaps from inaccurate temperature measurements. However, the Cu(2)-O(4) data vary more smoothly. Stern *et al.* also measured a fluctuation in the Cu(1)-O(4) broadening near T_c, however their measurement assumed a two-site distribution that had collapsed to one site in the same temperature range as the broadening fluctuation. Kimura *et al.*[42] measured a fluctuation in $\sigma_{\mathrm{Cu(1)-O(4)}}$ in a similar temperature range using a single O(4) site fit, but reported no anomalies in $\sigma_{\mathrm{Cu(2)-O(4)}}$ near T_c. No proven explanation of the physics behind these fluctuations exists, however, they can be interpreted in terms of changes in the correlation between the Cu and O atomic positions (see next section).

C. Correlations between atomic positions

Like the O(4)-site position, changes in ϕ with temperature can be attributed to changes in the static disorder of the individual sites, or to changes in the dynamics of the lattice displacements. As the temperature of the sample is decreased, static disorder could manifest itself as an ordering of oxygen vacancies, which would then generate a distinct set of positions for a given atom. If the site is split into two or three distinct positions, XAFS would measure an unusually broad peak for that pair and thus look like the atom-pair displacements are negatively correlated. It is therefore important to consider the absolute value of the broadening measurements from XAFS as compared to diffraction to try to help determine if the model used to fit the data is consistent, i.e., single atomic sites broadened harmonically around some average pair distance. Also, trends in the correlation with temperature should give some insight into which correlations within the unit cell are dependent on static or thermal disorder.

The most important result from the measurements of ϕ in Fig. 8 is that, within the estimated errors, they are all in the range from 0 to 1, indicating that the measurements of S_0^2, the calculated $F(k)$ and the model used to fit the data are all fairly accurate. More direct tests of the reliability of the absolute measurements of ϕ are provided by the nearest and the furthest bonds measured, that is, the Cu(1)-O(4) pairs and the Cu(1)-Cu(2) multiple scattering pair. Since the Cu(1)-O(4) pair is the nearest-neighbor pair in YBCO, we expect at low temperatures that ϕ should be very near unity, and it is:

$\phi_{Cu(1)-O(4)}$ demonstrates weak temperature dependence with a mean value of about 0.87, in approximate agreement with correlation measurements of the Hg-O(2) pair in Hg-1201.[50] The fluctuations near T_c are well within the increased errors after propagating the diffraction errors into ϕ.

The Cu(1)-Cu(2) atom pair is the furthest-neighbor fit and includes multiple scattering off the intervening O(4) atom. It is therefore a good test of the FEFF multiple-scattering calculations for $F(k)$,[34] as well as the absolute reliability of ϕ. We expect this pair to be the least correlated, and it is; $\phi_{Cu(1)-Cu(2)}$ shows no obvious change with temperature (although both XAFS and diffraction broadening factors show a significant temperature dependence) and is consistent with $\phi_{Cu(1)-Cu(2)} \cong 0$. The absolute accuracy of this pair is worse than the other pairs measured because the FEFF calculation includes multiple scattering off the O(4). Consequently, this measurement is consistent with $\phi_{Cu(1)-Cu(2)} \cong \pm 0.2$. The Cu-Ba pairs show a strong temperature dependence in ϕ, in each case dropping from about $\phi = 0.7$ to 0.5 between 20 and 200 K. The Cu(2)-Y pair is partially correlated ($\sim 0.45 \pm 0.1$) and shows little temperature dependence between 20–200 K. Perhaps surprisingly, the correlation coefficient for the cold temperature Cu(2)-Y pair is lower than the Cu-Ba pairs, even though the barium has the freedom to move along the *c* axis towards the chains without seriously distorting any bonds.

The most interesting correlation measurements are for the Cu(2)-O(4) pair. $\phi_{Cu(2)-O(4)}$ starts out very low (~ 0.4) but starts to *increase* to a maximum of ~ 0.6 just below T_c. In the vicinity of T_c, ϕ then drops to about 0.45 and then increases again to its maximum value of 0.6. As the temperature is increased above 100 K, ϕ decreases steadily from 0.6 to 0.4. This decrease in ϕ (and hence the increase in σ mentioned in Sec. VI B) may be the result of a negatively correlated mode being excited near T_c relative to the correlated mode that is dominating away from T_c. Such a mode may be consistent with a polaronic-hopping transport mode.[50]

VII. CONCLUSIONS

We have contrasted XAFS measurements on a thin film of YBCO on MgO with measurements on a single crystal with 1.4% Ni. We have also compared the results with a film on $LaAlO_3$, which gives essentially the same results for the O(4) distribution as the film on MgO, and with previous measurements on oriented powders. The single-crystal data exhibit an anharmonic site distribution for the O(4) atom which can be described as a split position below T_c and a single position above T_c. (The temperature range measured for the single crystal is limited.) This result is consistent with previous results on oriented powders.[5,9]

The main result of this paper is that the thin-film data show very different behavior. The O(4) peak can be well described by a single-site, harmonic distribution. This distribution does not show any strongly anharmonic behavior with temperature near T_c, or at any other temperature between 20–200 K.

These data refute the argument that the XAFS signal showing the split O(4) site distribution is too small to be measured reliably;[9] however, high S/N is required. The Fourier-filtered film data are very reproducible over the temperature range measured, and since only subtle changes occur in the O(4) site distribution for the film near T_c, the changes in the data with temperature are gradual and predominantly thermally driven. Because of this reproducibility, the rapidly changing XAFS from the single crystal must be taken as a legitimate signal, and not as noise.

Although we do not see any evidence of anharmonicity in the O(4) site in the film, fits show that the broadening factor for the Cu(2)-O(4) bond exhibits a local maximum above T_c followed by a drop below T_c to essentially its $T = 20$ K value. The Cu(1)-O(4) pair demonstrates similar behavior, but the effect is smaller and is not as systematic with temperature. Since there is no such behavior in the published diffraction literature[43,44] we have interpreted this as a change in the degree of correlation between the Cu(2) and the O(4) atoms, and possibly between the Cu(1) and the O(4) atoms. This result is in contrast to measurements by Kimura *et al.*[42] which show changes in the broadening factor for the Cu(1)-O(4) bond near T_c, but not in the Cu(2)-O(4) bond.

Finally, a better understanding of the local structure is obtained by considering the local correlations of the near neighbors. As mentioned above, the Cu(1)-O(4) is measured to be a very tight bond, yet the Cu(2)-O(4) is ''looser'' and exhibits a decrease in the correlation between the atoms near T_c, indicating that the chains act as a unit that is somewhat independent of the planes. This lack of correlation is also indicated by the measurement of the correlation coefficient $\phi_{Cu(1)-Cu(2)}$ near zero (< 0.2) that also does not change with temperature. However, the atomic displacements in the metal-oxide layer do become less correlated at higher temperatures. The atomic positions in the CuO_2 planes apparently remain correlated in the temperature range measured based on the measurements on the Cu(2)-Y atom pair.

ACKNOWLEDGMENTS

We wish to thank G. G. Li, E. D. Bauer, and Z. Kvitky for many useful discussions and for proofreading the manuscript. The experiments were performed at the Stanford Synchrotron Radiation Laboratory, which is operated by the U.S. Department of Energy, Division of Chemical Sciences, and by the NIH, Biomedical Resource Technology Program, Division of Research Resources. The work is supported in part by NSF Grant No. DMR-92-05204.

[1] J. G. Bednorz and K. A. Müller, Z. Phys. B **64**, 189 (1986).

[2] R. P. Sharma, L. E. Rehn, P. M. Baldo, and J. Z. Liu, Phys. Rev. Lett. **62**, 2869 (1989).

[3] R. P. Sharma, L. E. Rehn, P. M. Baldo, and J. Z. Liu, Phys. Rev. B **40**, 11 396 (1989).

[4] P. M. Horn, D. T. Keane, G. A. Held, J. L. Jordan-Sweet, D. L. Kaiser, F. Holtzberg, and T. M. Rice, Phys. Rev. Lett. **59**, 2772 (1987).

[5] J. Mustre de Leon, S. D. Conradson, I. Batistic, and A. R. Bishop, Phys. Rev. Lett. **65**, 1675 (1990).

[6] J. Mustre de Leon, S. D. Conradson, I. Batistic, A. R. Bishop, I. D. Raistrick, M. C. Aronson, and F. H. Garzon, Phys. Rev. B **45**, 2447 (1992).
[7] H. You, U. Welp, and Y. Fang, Phys. Rev. B **43**, 3660 (1991).
[8] C. Meingast, O. Kraut, T. Wold, H. Wühl, A. Erb, and G. Müller-Vogt, Phys. Rev. Lett. **67**, 1634 (1991).
[9] E. A. Stern, M. Qian, Y. Yacoby, S. M. Heald, and H. Maeda, Physica C **209**, 331 (1993).
[10] D. Mihailovic, K. F. McCarty, and D. S. Ginley, Phys. Rev. B **47**, 8910 (1993).
[11] D. Emin, in *Condensed Matter Physics: The Theodore D. Holstein Symposium*, edited by R. L. Orback (Springer-Verlag, New York, 1986), pp. 16–34.
[12] D. Emin, in *Lattice Effects in High-T_c Superconductors*, edited by Y. Bar-Yam, T. Egami, J. Mustre-de Leon, and A. R. Bishop (World Scientific, River Edge, NJ, 1992), pp. 377–388.
[13] J. Ranninger and U. Thibblin, Phys. Rev. B **45**, 7730 (1992).
[14] J. R. Hardy, J. W. Flocken, and R. A. Guenther, in *Lattice Effects in High-T_c Superconductors* (Ref. 12), pp. 327–339.
[15] J. Röhler, in *Materials and Crystallographic Aspects of High-T_c Superconductivity, Proceedings of the 20th course of the International School of Crystallography*, edited by E. Kaldis (Kluwer Academic, Boston, 1994).
[16] T. Zeiske, R. S. D. Hohlwein, N. H. Anderson, and T. Wolf, Nature (London) **353**, 542 (1991).
[17] T. Zeiske, D. Hohlwein, R. Sonntag, F. Kubanek, and G. Collin, Z. Phys. B **86**, 11 (1992).
[18] P. Bordet, C. Chaillout, T. Fournier, M. Marezio, E. Kaldis, J. Kaldis, J. Karpinski, and E. Jilek, Phys. Rev. B **47**, 3465 (1993).
[19] B. H. Toby, T. Egami, J. D. Jorgensen, and M. A. Subramanian, Phys. Rev. Lett. **64**, 2414 (1990).
[20] P. G. Allen, J. Mustre de Leon, S. D. Conradson, and A. R. Bishop, Phys. Rev. B **44**, 9480 (1991).
[21] B. M. Lairson, Ph.D. thesis, Stanford University, 1991.
[22] C. B. Eom, J. Z. Sun, B. M. Lairson, S. K. Streiffer, A. F. Marshal, K. Yamamoto, S. M. Anlage, J. C. Bravman, and T. H. Geballe, Physica C **171**, 354 (1990).
[23] F. Bridges, J. B. Boyce, T. Claeson, T. H. Geballe, and J. M. Tarascon, Phys. Rev. B **42**, 2137 (1990).
[24] P. Schleger, W. N. Hardy, and B. X. Yang, Physica C **176**, 261 (1991).
[25] R. Liang, P. Dosanjh, D. A. Bonn, D. J. Baar, J. F. Caolan, and W. N. Hardy, Physica C **195**, 51 (1992).
[26] F. Bridges, G. G. Li, and X. Wang, Nucl. Instrum. Methods Phys. Res. Sect. A **320**, 548 (1992).
[27] G. G. Li, F. Bridges, and X. Wang, Nucl. Instrum. Methods Phys. Res. Sect. A **340**, 420 (1994).
[28] T. M. Hayes and J. B. Boyce, in *Solid State Physics*, edited by H. Ehrenreich, F. Seitz, and D. Turnbull (Academic, New York, 1982), Vol. 37, p. 173.
[29] G. G. Li, F. Bridges, and C. H. Booth, Phys. Rev. B **52**, 6332 (1995).
[30] F. Bridges, C. H. Booth, and G. G. Li, Physica B **208&209**, 121 (1995).
[31] J. Boyce, F. Bridges, T. Claeson, R. S. Howland, and T. H. Geballe, Phys. Rev. B **36**, 5251 (1987).
[32] E. D. Crozier, N. Alberding, K. R. Bauchspiess, A. J. Seary, and S. Gygax, Phys. Rev. B **36**, 8288 (1987).
[33] J. Boyce, F. Bridges, T. Claeson, and M. Nygren, Phys. Rev. B **39**, 6555 (1989).
[34] J. J. Rehr, R. C. Albers, and S. I. Zabinsky, Phys. Rev. Lett. **69**, 3397 (1992).
[35] S. I. Zabinsky, A. Ankudinov, J. J. Rehr, and R. C. Albers, Phys. Rev. B **52**, 2995 (1995).
[36] S. I. Zabinsky, Ph.D. thesis, University of Washington, 1993.
[37] B. K. Teo, *EXAFS: Basic Principles and Data Analysis* (Springer-Verlag, New York, 1986).
[38] L. Tröger, D. Arvanitis, K. Barberschke, H. Michaelis, U. Grimm, and E. Zschech, Phys. Rev. B **46**, 3283 (1992).
[39] E. A. Stern, Phys. Rev. B **48**, 9825 (1993).
[40] P. Eisenberger and G. S. Brown, Solid State Commun. **29**, 418 (1979).
[41] W. H. Press, B. P. Flannery, S. A. Teukolsky, and W. T. Vetterling, in *Numerical Recipes: The Art of Scientific Computing*, 1st ed. (Cambridge University Press, New York, 1986), pp. 457,458.
[42] H. Kimura, H. Oyanagi, T. Terashima, H. Yamaguchi, Y. Bando, and J. Mizuki, Jpn. J. Appl. Phys. **32-2**, 584 (1993).
[43] R. P. Sharma, F. J. Rorella, J. D. Jorgensen, and L. E. Rehn, Physica C **174**, 409 (1991).
[44] G. H. Kwei, A. C. Larson, W. L. Hults, and J. L. Smith, Physica C **169**, 217 (1990).
[45] S.-G. Lee, S. C. Bae, J. K. Ku, and H. J. Shin, Phys. Rev. B **46**, 9142 (1992).
[46] B. Pashmakov, K. Zhang, H. M. Jaeger, P. Tiwari, and X. D. Wu, Physica C **249**, 289 (1995).
[47] D. Mihailovic, C. M. Foster, K. F. Voss, T. Mertelj, I. Poberaj, and N. Herron, Phys. Rev. B **44**, 237 (1991).
[48] J. H. Nickel, D. E. Morris, and J. W. Ager, Phys. Rev. Lett. **70**, 81 (1993).
[49] H.-G. Lee, H.-S. Shin, I.-S. Yang, J.-J. Yu, and N. H. Hur, Physica C **233**, 35 (1994).
[50] C. H. Booth, F. Bridges, E. D. Bauer, G. G. Li, J. B. Boyce, T. Claeson, C. H. Chu, and Q. Xiong, Phys. Rev. B **52**, 15 745 (1995).
[51] J. Mustre de Leon, I. Batistic, A. R. Bishop, S. D. Conradson, and I. D. Raistrick, Phys. Rev. B **47**, 12 322 (1993).